

Surface superconductivity and H_{c3} in UPt_3

Ding Chuan Chen and Anupam Garg

Department of Physics and Astronomy and Materials Research Center,

Northwestern University, Evanston, Illinois 60208

(February 21, 2022)

Abstract

Surface superconductivity is studied within Ginzburg-Landau theory for two classes of models for the order parameter of UPt_3 . The first class assumes two independent one-dimensional order parameters (AB models), while the second assumes a single two-dimensional order parameter (E models). H_{c3} is calculated for all cases where the surface normal and magnetic field lie along high symmetry directions. Assuming specular reflection, it is found that except when $H \parallel \hat{c}$, the ratio H_{c3}/H_{c2} is either unity or equals its 's-wave' value 1.695, although the precise H_{c3} vs. T curve predicted by the AB and E models differs for various geometries. The results are compared with recent experiments, and predictions are made for future experiments.

PACS numbers: 74.60.Ec, 74.70.Tx, 74.20.De, 74.60.-w

I. INTRODUCTION

UPt₃ is generally believed to be a reduced symmetry superconductor, i.e., one that breaks rotational and/or time reversal symmetries of the normal state, in addition to the U(1) gauge symmetry [1,2]. The strongest basis for this belief is the phase diagram which displays multiple superconducting phases [3{8], just as liquid ³He has multiple superfluid phases. In this paper we shall study surface superconductivity in UPt₃, and see if competing models make differing predictions which might be experimentally tested.

We briefly review the existing models for the order parameter in UPt₃. There are two main classes. The first class, which we shall refer to as E' models [1,9{13], entails a single two-component order parameter, which may belong to any of the two-dimensional representations (E_{1g}, E_{2g}, E_{1u}, E_{2u}) of D_{6h}⁰, the point group of normal UPt₃ [14]. The second class of models posits two independent order parameters belonging to different representations [12,15{18]. In one subclass [19], which can be analyzed in great detail, comprising what we shall call AB' models, both order parameters have the same parity; one transforms as an A representation and the other as a B representation of D_{6h}⁰. Thus, if the common parity is even [20], the pair of order parameters transforms in one of four possible ways: (A_{1g}, B_{1g}), (A_{1g}, B_{2g}), (A_{2g}, B_{1g}), (A_{2g}, B_{2g}). This division into two classes is useful because in the simplest form of Ginzburg-Landau (GL) theory in which only terms that are formally of order (1 - T/T_c)² are kept, all E models have the same formal GL free energy, and all AB models have the same GL free energy. This leads one to sometimes refer to them in the singular as the E model or the AB model.

The E model invokes a symmetry breaking field (SBF), usually taken to be a weak antiferromagnetism that sets in at 5 K [21,22], in order to split the superconducting transition in zero field into two transitions as observed. The AB model posits two nearby transition temperatures by fiat. The original version of the E model was shown to be incompatible [13,15] with experiments in that it fails to yield a tetracritical point in the H-T plane for H \parallel k_c [23]. (Whether there is or is not a true tetracritical point in the experimentally

observed phase diagram is irrelevant. At the very least one has two phase boundaries $H_{c2}(T)$ and $H_{ci}(T)$ that approach within 10–15 mK of one another, and the outermost line $H_{c2}(T)$ has a sharp change in the sign of the curvature near this apparent tetracritical point. The theory can not explain this ‘near collision’ either.) This led us to propose the AB model which does not have this flaw. Our proposal in turn led Sauls to propose a refinement of the E model [1], which has three ingredients: (i) a specific E_{2u} order parameter (see below), (ii) a nearly cylindrically symmetric Fermi surface, and (iii) coupling of the gradient terms in the GL free energy to the SBF. A cylindrical Fermi surface causes the dangerous gradient coupling terms in the free energy [23] to vanish within weak coupling BCS theory for an E_2 order parameter, and in conjunction with ingredient (iii) restores the tetracritical point for $H_{k\hat{c}}$.

In this paper we shall use GL theory to calculate H_{c3} for UPT_3 within the original E model and the AB model. The GL free energy for the refined E model is mathematically isomorphic to, and can be regarded as a special case of, the AB model free energy [24]. Since the key issue that determines H_{c3} is the boundary condition on the order parameter, however, the refined E_{2u} model of Sauls will have the same $H_{c3}(T)$ curves as the unreduced E_{2u} model for $H_{k\hat{c}}$. Indeed, H_{c3} curves may be similar for these two models even when $H_{k\hat{c}}$, except that one must beware of kinks in the refined model. We will limit ourselves to cases where the field H and the surface normal \hat{n} lie in high crystal symmetry directions or planes. Further, we only consider ideal, or specularly reflecting surfaces.

The motivation for this study is that we expect qualitative differences in the behavior of H_{c3} between the various models for various geometries. Firstly, the boundary conditions are different amongst the E models, leading to differences in H_{c3} . Secondly, in the AB model the eigenvalue equations for H_{c3} decouple into separate equations for two components, and whenever the surface supports both components, the H_{c3} curve is expected to mirror H_{c2} and show a kink. In the E model, on the other hand, even for $H_{k\hat{c}}$, the gradient terms can couple the two components. It is thus possible for the kink in H_{c3} to be smoothed out. We shall see that whether this happens or not is a question of dynamics, not symmetry.

In fact, there turns out to be no smoothing with the gradient coupling values we use. A short quantitative estimate of this effect seems to be hard to get, however, so we present the full analysis which follows. Since an experimental measurement of H_{c3} has now been reported [25] for some of the geometries that we study, we can use our results to restrict the acceptable order parameters for UPt_3 . We also hope that our work will spur a more detailed experimental study of H_{c3} in other geometries as well, as this will sharpen our understanding of the order parameter even further.

We note here that as this paper was being written, we learned of a recent paper by Samokhin [26], also discussing H_{c3} in UPt_3 within E models. Samokhin gives a microscopic foundation to the boundary conditions on the order parameter [27], while we take a purely phenomenological approach. Further, he focuses on the case where $H \parallel \hat{c}$, and the surface normal is arbitrarily oriented in the a - b plane. We have largely avoided detailed study of the $H \parallel \hat{c}$ geometry because of the problems it presents in comparing to the observed bulk upper critical field. Thus Samokhin's work is nicely complementary to ours.

The rest of the paper is organized as follows. In Sec. II, we recapitulate the bare essentials of the theory of surface superconductivity for fully symmetric superconductors with a complex scalar order parameter, paying special attention to the boundary conditions. We then extend these ideas to the AB and E models. The case of the E model is rather rich. Depending on the exact order parameter and field and surface orientation, the surface may or may not suppress superconductivity. We tabulate these cases and proceed to study them in Secs. III and IV. Certain technical aspects of the calculations are given in the Appendix. In Sec. V, we compare our results with the experiments of Keller et. al. [25], and see which order parameters are compatible. Our results are summarized in Table III, and the reader who is not interested in the details of the analysis should skip to that directly. We conclude with suggestions for future work.

II. BASIC THEORY OF SURFACE SUPERCONDUCTIVITY

A. Fully symmetric superconductors

We first recapitulate the theory for a superconductor with a complex scalar order parameter ψ , occupying the half space $z \geq 0$ [28{30]. H_{c3} is found by solving the linearized GL equation

$$\frac{1}{2m} \left(-\hbar^2 \nabla^2 - \frac{2e}{c} A \right) \psi = 0 \quad (T) \quad (2.1)$$

subject to the boundary condition of no current flow across the surface: $j_z = 0$. The notation in Eq. (2.1) is standard.

If $H < H_{c2}$, then there is no surface superconductivity, and technically $H_{c3} = H_{c2}$. The problem is more interesting when $H > H_{c2}$. For an interface with a vacuum or insulator, the boundary condition $j_z = 0$ becomes

$$D_z \psi|_{z=0} = 0 \quad (2.2)$$

where D is the gauge covariant derivative. Taking $A = H z \hat{y}$, and writing ψ as a plane wave in the x-y plane with wavevector $(k_x; k_y)$ times a function $f(z)$, Eqs. (2.1) and (2.2) can be rewritten as

$$\left[\frac{d^2}{dz^2} + \frac{2}{\xi_0^2} (z - z_0)^2 + k_x^2 \right] f = \frac{1}{2(T)} f; \quad (2.3)$$

with $(df/dz)_{z=0} = 0$. Here, $z_0 = k_y \xi_0^2 / 2H$, ξ_0 is the flux quantum, and $(T) = \hbar^2 / 2m(T)$. The highest field eigenvalue is obtained with $k_x = 0$, and

$$z_0 = g_0(T); \quad H_{c3} = \frac{1}{g_0} H_{c2} \quad (2.4)$$

with $g_0 = 0.59010$. ($1/g_0 = 1.6946$.) Recall that $H_{c2} = hc / 2e(T)$:

Kittel's variational solution to the above problem is also worth reproducing. Taking

$$f = (2 - z^2)^{1/4} \exp(-z^2/4\xi_0^2) \quad (2.5)$$

and minimizing the total energy with respect to z_0 and ξ_0 gives

$$\begin{aligned} \kappa^2 &= \frac{1}{2g_k} \kappa^2(T); \\ z_0 &= (\kappa^2)^{1/2} = 0.727(T); \\ H_{c3} &= g_k^{-1} H_{c2}; \end{aligned} \tag{2.6}$$

with $g_k = (1 - \kappa^2)^{-1/2} = 0.603$. ($1/g_k = 1.66$.) Note that this variational solution has the property of zero integrated current in the y direction:

$$\int_0^{z_1} j_y dz / \int_0^{z_1} (z - z_0) f^2(z) dz = 0; \tag{2.7}$$

Finally, we note that if Eq. (2.2) is replaced by the boundary condition $\psi(0) = 0$, the highest H_{c3} eigenvalue is obtained by letting $z_0 \rightarrow 1$ in Eq. (2.3), and $H_{c3} = H_{c2}$.

B. Reduced symmetry superconductors

For both E and AB models, the order parameter can be written as a two-component complex vector

$$\psi = \begin{pmatrix} \psi_1 \\ \psi_2 \end{pmatrix} = \psi_0 \begin{pmatrix} 1 \\ \alpha \end{pmatrix} \tag{2.8}$$

This transforms as a single irreducible (E) representation of D_{6h}^0 in the E model and as a reducible representation in the AB case. The quadratic part of the GL free energy density (which is all that matters for H_{c3}) can be written compactly as

$$f_{GL}^{(2)} = \sum_{r=1,2} \kappa_r(T) j_r^2 + \sum_{i,j;r;s} \gamma_{ij}^{rs} (\nabla_i \psi_r) (\nabla_j \psi_s); \tag{2.9}$$

where $i, j \in \{x, y, z\}$, and the γ 's are gradient coefficients suitably constrained by symmetry.

It follows from Eq. (2.9) that the current is given by

$$j_i = \frac{4e}{h} \text{Im} \sum_{j;r;s} \gamma_{ij}^{rs} \psi_r \nabla_j \psi_s; \tag{2.10}$$

At first sight the condition $j \cdot \hat{n} = 0$ cannot be written as a linear equation in ψ . Just as in the case of ordinary superconductors, however, a linear equation can be obtained [26], as was first done for $^3\text{He-A}$ [31]. In contrast to ordinary superconductors, the roughness

of the interface is now very important. A rough surface is in general pair breaking. Since we wish to study the maximum possible enhancement of H_{c3} , we will only consider ideal or specularly reflecting surfaces. Further, as mentioned before, we shall only consider cases where the surface normal \hat{n} and the field H lie in high symmetry directions or planes. Under these conditions, the microscopic analyses [26,27,31], which we shall not repeat, show that the boundary condition on each component of ψ reduces to [32]

$$\psi_r = 0 \text{ or } (\hat{n} \cdot \nabla)_r \psi = 0: \quad (2.11)$$

Note that both components need not obey the same condition; one could have $\psi_1 = 0$ and $(\hat{n} \cdot \nabla)_2 \psi = 0$. The general rule can be written as follows. Let us write the momentum-space gap function in the Balian-Werthamer notation,

$$\psi_0(\mathbf{k}) = \sum_{r=1}^X \psi_r(\mathbf{k}); \quad (\text{even parity}); \quad (2.12)$$

$$\vec{\psi}(\mathbf{k}) = \sum_{r=1}^X \vec{\psi}_r(\mathbf{k}); \quad (\text{odd parity}); \quad (2.13)$$

where ψ_r or $\vec{\psi}_r$ are basis functions of the appropriate representation. Note that in the odd parity case, $\vec{\psi}$ and $\vec{\psi}_r$ are vectors in pseudo-spin space. The precise boundary conditions in Eq. (2.11) are then as follows. Let us denote by $R\mathbf{k}$ the wave vector obtained from \mathbf{k} by reflection in the plane normal to \hat{n} . Then, in the even parity case, at the surface we have,

$$\psi_r = 0 \quad \text{if} \quad \psi_r(R\mathbf{k}) = \psi_r(\mathbf{k}); \quad (2.14)$$

$$(\hat{n} \cdot \nabla)_r \psi = 0 \quad \text{if} \quad \psi_r(R\mathbf{k}) = + \psi_r(\mathbf{k}): \quad (2.15)$$

The surface acts in effect as a momentum space mirror. If this mirror plane is a nodal plane for ψ_r , then ψ_r must vanish at the surface. If the mirror plane is antinodal, then the normal derivative must vanish. In the odd parity case, we replace ψ_r by $\vec{\psi}_r$. As noted in Ref. [33], it is unlikely that in reality $\vec{\psi}_r$ will be exactly odd or even under reflection normal to any \hat{n} , even those of high symmetry, as the surface will in general be pseudospin. Keeping our goal of studying surface superconductivity under idealized or optimal conditions in mind, we shall ignore this complication.

In Table I we give a few illustrative cases of boundary conditions obtained by applying the above rule to candidate order parameters for UPt_3 . Since we will always take $H_{\hat{n}} = 0$, it is always possible to choose $A \cdot \hat{n}$, and the boundary condition (2.15) reduces to $r_{\hat{n}} = 0$. Several points about this table should be noted: (i) The directions x, y, z are fixed along the crystal symmetry directions with $\hat{x} = \hat{a}$, $\hat{y} = \hat{b}$, and $\hat{z} = \hat{c}$. (ii) For odd parity, unit vectors in pseudospin space are denoted by a subscript \mathcal{S}' . (iii) For each representation we have generally given the simplest possible basis function. As noted in Ref. [33] this does not yield the most general gap function allowed by symmetry. As a counter-example, we show two order parameters for E_{2u} [34], distinguished by superscripts. The second of these is in fact the one advanced by Sauls [1] and by Norman [35]. (iv) In each case, we list the pair of quantities that must vanish at the interface. Thus for the E_{2g} example, with $\hat{n} = \hat{x}$, we must have $\psi_1 = \psi_2 = 0$. (v) In some cases, the boundary conditions are mixed, i.e. of the type discussed in Refs. [26,32].

The reader can write down the correct boundary conditions for any other order parameter using our rules. In subsequent sections, we will solve the H_{c3} problem for both AB and E-type models. In the case of the AB models, H_{c3} is independently found for the A and B component. By a simple rescaling of the coordinates, the eigenvalue equation can be reduced to that of the isotropic case. The boundary condition is either $r = 0$ or $\psi_r = 0$, yielding $H_{c3} = H_{c2}$ equal to 1 or g_0^{-1} , respectively. Having found $H_{c3}(T)$ in this manner for each component separately, the thermodynamic $H_{c3}(T)$ is taken to be the larger of the two for each value of T . A similar procedure will turn out to work in many cases for the E-models, although it is not obvious a priori that the equations for ψ_1 and ψ_2 will decouple.

III. H_{c3} FOR AB MODELS

In this section we will calculate H_{c3} for the AB model order parameters listed in Table I. Writing $(\psi_a; \psi_b)$ instead of $(\psi_1; \psi_2)$, the free energy (to quadratic order in ψ) for all AB models is given by

$$f_{GL}^{(2)} = \sum_{r=a,b} \left(\frac{X}{r} j_r j_r^2 + \frac{D}{r} j_r^2 + \frac{D_0}{r} j_z j_r^2 \right) \quad (3.1)$$

Here $r = 0(T - T_r)$, and all r 's are positive. We assume that a and b belong to the A and B representations, respectively.

$$A \cdot \hat{n} = \hat{z}$$

Since all directions of $H \cdot \hat{n}$ are equivalent, let us take $H = H \hat{x}$, $A = H z \hat{y}$. Minimization of $f_{GL}^{(2)}$ leads to the GL equations, which decouple for a and b :

$$r^4 \frac{\partial^2}{\partial x^2} + \frac{\partial}{\partial y} + \frac{2ie}{hc} H z^3 \frac{\partial}{\partial z} - r \frac{\partial^2}{\partial z^2} = 0 \quad (3.2)$$

The boundary conditions are $\partial_z a = \partial_z b = 0$ at $z = 0$.

Equation (3.2) can clearly be made isotropic by a rescaling of coordinates. We then get

$$H_{c3}^a(T) = 1.695 H_{c2}^a(T); \quad (3.3)$$

$$H_{c3}^b(T) = H_{c2}^b(T); \quad (3.4)$$

where the superscript labels the order parameter component that is nucleating.

Taking the $H_{c2}(T)$ curves to have a kink as seen experimentally, we obtain a very simple picture for H_{c3} . For the even parity case, if $T_a > T_b$, there is only one branch to $H_{c3}(T)$, and it onsets at T_a , i.e., the upper transition in zero field. If $T_b > T_a$, there is again only one branch, but it onsets below the upper transition temperature, and it extrapolates to T_b for $H = 0$. These possibilities are shown schematically in Figs. 1 and 2. For the odd parity cases, the roles of a and b are reversed, i.e., Fig. 1 applies if $T_b > T_a$, and Fig. 2 applies if $T_a > T_b$.

$$B \cdot \hat{n} = \hat{x} \text{ or } \hat{n} = \hat{y}$$

Let us first consider the $A_{1g} - B_{2g}$ order parameter. If we take $\hat{n} = \hat{x}$; $H = H \hat{y}$, the analysis is identical to that just given, and we recover Figs. 1 and 2 for $T_a > T_b$ and $T_b > T_a$ respectively. If $\hat{n} = \hat{y}$, and $H = H \hat{x}$, say, then taking $A = H y \hat{z}$, the GL equation becomes

$$r \frac{\partial^2}{\partial x^2} + \frac{\partial^2}{\partial y^2} - r \frac{\partial}{\partial z} - \frac{2ie}{hc} H_y r = r r; \quad (3.5)$$

which can be isotropized as before, but the boundary conditions now are $\partial_z a = \partial_z b = 0$ at $z = 0$, so H_{c3} is given by

$$H_{c3}^r(T) = 1.695 H_{c2}^r(T); \quad r = a, b; \quad (3.6)$$

The resulting picture is shown in Fig. 3. Note that within the GL approximation, the H_{c3} and H_{c2} kinks occur at the same temperature, as can be proved by simple geometry. Further, in this case, we expect to see inner transition lines analogous to those for H_{c2} , corresponding to the onset of surface superconductivity in the other component.

We get the same answers as above for the $A_{1u} - B_{1u}$ case, as the boundary conditions are the same. For the $A_{1u} - B_{2u}$ order parameter, the results for the $\hat{n} = \hat{x}$ and the $\hat{n} = \hat{y}$ cases are interchanged.

IV. H_{c3} FOR E MODELS

We turn at last to our main problem, namely that of H_{c3} for the E models. For the reasons mentioned in Sec. I, we will not consider explicitly the refinements made by Sauls [1].

The free energy for all E models is more conveniently represented by regarding $(\phi_1; \phi_2)$ as the components of a vector in the x, y plane. This is self-evident for the E_1 cases, but as shown by Tokuyasu [36], the number and form of the invariants is the same for the E_2 cases as well. Writing $(\phi_1; \phi_2)$ as $(\phi_x; \phi_y)$, we can write the quadratic part of f_{GL} as

$$f_{GL}^{(2)} = \phi_x^2 + \phi_y^2 + D_{ij} \phi_i \phi_j + D_{11} \phi_x^2 + D_{22} \phi_y^2 + D_{12} \phi_x \phi_y + D_{31} \phi_x^2 + D_{32} \phi_y^2; \quad (4.1)$$

where, $i, j = x, y$, and we sum over repeated indices. Also, we have $D_{ij} = D_{ji}(T - T_0)$, with $T = T_{c0} = 0$.

We write the GL equations implied by Eq. (4.1) using the notation of Ref. [37]. We scale all lengths by $l = (hc/2eH)^{1/2}$, T_0 and ϕ_0 by $\phi_0 = \phi_0^2$ with $\phi_0 = \phi_0^2 + (\phi_0^2)^2$, and

$$w > 0; 1 - v > 0; 1 + v > 2|j| \tag{4.5}$$

It follows from these that $|j| < 1$. Secondly, the $H_{\hat{z}}$ case involves w and u , but only $|j|$ can be found from experimental $H_{\hat{z}}$ slopes. (The $H_{\hat{k}}$ case involves only v , but comparison with experiment is problematic as discussed in Section I.) The values of u so determined vary quite a bit. We shall take $|j| = 0.46$ in our numerical work in accord with the data of Ref. [3].

$$A \cdot \hat{n} = \hat{z}, H_{\hat{z}}$$

Because of basal plane isotropy, we expect the same $H_{\hat{z}}$ curve for all field orientations in this case. Let us take $H_{\hat{k}}$, $\theta > 0$, and let us work in the gauge $A = H_{\hat{z}} \hat{y}$. Then in Eq. (4.3), $p_z = \partial_z$, $p_x = \partial_x$, $p_y = \partial_y + z$. We can clearly take ψ as a plane wave in the x-y plane and replace p_x by k and p_y by $z_0 - z$, where k and z_0 are wavevector components. Then, $f_{p_x; p_y} = 2k(z - z_0)$, and we get a one-dimensional Hamiltonian,

$$H_{GL} = \frac{1}{2} w \partial_z^2 + (1 - u)(z - z_0)^2 + (1 + u)k^2 + \dots + 2ku(z - z_0) \tag{4.6}$$

For the E_{2g} , E_{1u} , and $E_{2u}^{(1)}$ cases listed in Table I, the boundary conditions are $\partial_z \psi = \partial_z \psi = 0$ at $z = 0$. If $k = 0$ for all T , we get two decoupled $H_{\hat{z}}$ problems and a kink in $H_{\hat{z}}$ as in Fig. 3. The only nontrivial features arise from the possibility of having $k \neq 0$. Such k -mixing is found to affect the $H_{\hat{z}}$ curves for $u = 0.61$ for basal plane fields [37]. Whether the lowest energy eigenvalue for the $H_{\hat{z}}$ problem ever corresponds to $k \neq 0$ is a dynamical question, to which we have not been able to find a two-line answer. It is obvious that having $k \neq 0$ raises the energy from the diagonal terms in Eq. (4.6). The compensation of this rise from the off-diagonal terms is likely to be largest when the x and y solutions are nearly degenerate, i.e. for fields near the kink found with $k = 0$. If the energy were lowered by having $k \neq 0$, the crossing of the x and y solutions would turn into an anticrossing, and the kink would be smoothed out. Our goal is to explore this possibility.

It is clear from Eq. (4.6), that a $k \neq 0$ solution is more favored for large values of u . Let us mention two obvious analytic approaches to this problem. Firstly, a lower bound on the minimum u required can be found by constructing a Schwarz inequality for the matrix element of the off-diagonal term in Eq. (4.6), but this bound is too small to be useful. Secondly, one might try and construct variational solutions analogous to Eq. (2.5), with different widths x and y for ψ_x and ψ_y . The energy is then a function of five variational parameters, x, y, z_0, k , and a mixing angle, and the minimization is complicated enough that one might as well attempt a nonvariational numerical solution. This approach does reveal one fact, however. If u is small, x and y are likely to be similar, and Eq. (2.7) shows that the matrix element of $(z - z_0)$ is likely to be small. Thus the effect of the off-diagonal terms in Eq. (4.6) is probably of $O(u^2)$.

We have therefore solved the eigenvalue problem for H_{c3} numerically. We do this by working in a basis of harmonic oscillator eigenfunctions with unequal length scales ($w = (1/u)^{1/4}$ for x and y). Only even parity (about $z = 0$) functions are used in accord with the boundary conditions. The Hamiltonian (4.6) is almost diagonal in this basis. The evaluation of the off-diagonal terms is described in the Appendix. We find the lowest eigenvalue E_{min} and associated eigenfunction ψ_{min} of H_{GL} numerically for given k and z_0 , and minimize with respect to k and z_0 via the conjugate gradient method. The required gradients are efficiently found using the identity

$$\frac{\partial}{\partial k} E_{min} = \int \psi_{min} \frac{\partial H_{GL}}{\partial k} \psi_{min} ; \quad (4.7)$$

and a similar one for the z_0 derivative. These calculations are done for \tilde{u} ranging from 0.1 to 10. This range is large enough to encompass the kink region comfortably, as all terms in Eq. (4.6) are of order unity.

We find that for $u = 0.46$, k is numerically equal to zero for all \tilde{u} values considered. In fact, k -mixing occurs only for $u > 0.59$, but the resulting anticrossing is very narrow, and substantial curvature in $H_{c3}(T)$ is only visibly evident for $u > 0.8$. Thus, for experimentally relevant values of u , the picture for H_{c3} is the same as in Fig. 3, i.e., the $H_{c3} = H_{c2}$ ratio is

always ideal and there is a kink in H_{c3} [41]. Once again, we expect to see inner H_{c3} lines which we have not explicitly calculated.

The H_{c3} problem is trivial for the E_{1g} and the $E_{2u}^{(2)}$ cases listed in Table I. The boundary conditions now are $x = y = 0$ at $z = 0$, and the surface cannot support superconductivity, i.e., $H_{c3} = H_{c2}$.

B. $\hat{n} \parallel \hat{z}$, $H \parallel \hat{z} \perp \hat{n}$

In this geometry, as can be seen from Table I, except for the $E_{2u}^{(1)}$ order parameter, the boundary conditions call for only one of the ψ_i to vanish at the surface. The other component is not suppressed by the surface. The form of $H_{c3}(T)$ is different depending on whether the surface suppressed component has the higher or lower transition temperature. This in turn depends on the sign of the coupling of the symmetry breaking field (SBF) to the order parameter.

To understand this point, let us first consider the E_{1g} and E_{1u} cases from Table I. The two high-symmetry geometries are shown in Fig. 4. For cases (a) and (b), we have $M^y \parallel k \hat{x}$ or $M^y \parallel k \hat{y}$, and $\psi = \psi^y$ or $\psi = \psi^x$, respectively. Suppose $\alpha > 0$. Then, for the case of Fig. 4(a) we have $\psi^y = 0$ and $\alpha < 0$, i.e., ψ^y has the lower T_c . For the case of Fig. 4(b) we have $\psi^x = 0$ and $\alpha > 0$, i.e., ψ^x has the lower T_c . In both geometries, the surface and the SBF act in opposition, i.e., the SBF is oriented so that the surface supported order parameter component has the lower T_c . In contrast, if $\alpha < 0$, then the surface and the SBF act in concert, and the surface supported component has higher T_c .

The sign of α is unknown and fixed by microscopic physics. We can conclude, though, that whether the surface and SBF act in concert or opposition, for E_1 order parameters, the same behavior will be seen for the two geometries in Fig. 4. This point can be understood as follows. An E_1 order parameter behaves as a vector in the x - y plane, and so if we rotate the surface normal \hat{n} , keeping $H \parallel k \hat{z} \perp \hat{n}$, the boundary conditions on ψ rotate in the same way, and we get an isotropic H_{c3} .

For the E_{2g} and $E_{2u}^{(2)}$ order parameters, we can see from Table I that the same component, x , is supported by the surface for both $\hat{n} = \hat{x}$ and $\hat{n} = \hat{y}$. For any $\text{sgn}(\)$, this component must have the lower T_c for one orientation, and the higher T_c for the other, leading to different answers for H_{c3} . In terms of symmetry, this can be understood by saying that as \hat{n} is rotated in the basal plane, an E_2 order parameter rotates at twice the rate of a vector. Denoting the angle between \hat{n} and \hat{x} by θ , the boundary conditions change with θ , reversing every 30° . Thus the SBF and the surface will act in concert for one geometry in Fig. 4, and in opposition for the other.

We study the cases of surface and SBF in concert and in opposition separately below. It is convenient to $x \sim > 0$, so that y always has the higher T_c , and to rotate \hat{n} and H as needed.

1. Surface and SBF in concert

We take the geometry of Fig. 4 (a), and $\frac{\partial}{\partial y} = \frac{\partial}{\partial x} = 0$ at $x = 0$. We also take $A = Hx^2$, allowing us to put $p_z = (i\partial_z + x)$, $p_x = i\partial_x$, $p_y = i\partial_y$ in Eq. (4.3). Further taking as a plane wave in the yz plane, we can replace p_y by k , p_z by $(x - x_0)$, and $p_x; p_y$ by $2ik\partial_x$. (Obviously, k and x_0 are wavevector components.) The resulting one dimensional GL Hamiltonian is

$$H_{GL} = \frac{1}{4} \left[(1+u)\partial_x^2 + (1-u)k^2 + w(x-x_0)^2 + \frac{2iuk\partial_x}{(1-u)\partial_x^2 + (1+u)k^2 + w(x-x_0)^2} \right] \quad (4.8)$$

If $k = 0$, we get two decoupled problems, and because of the boundary conditions $H_{c3}^y = 1/69H_{c2}^y$, $H_{c3}^x = H_{c2}^x$. This leads to the phase diagram of Fig. 1.

Thus, as in subsection A, the only real question is whether $k \neq 0$ gives a lower energy. We have diagonalized H_{GL} numerically using a harmonic oscillator wavefunction basis with length scales $[(1-u)/w]^{1/4}$, and odd and even parities about $x = 0$, for x and y respectively. The calculation is done as in subsection A, and we again find that with $u = 0.46$, $k = 0$

for all values of $\tilde{\mu}$ [42]. The H_{c3} picture is that of Fig. 1.

2. Surface and SBF in opposition

We take the geometry of Fig. 4 (b), and $\psi_y = \psi_x^0 = 0$ at $y = 0$. Further, with $A = H_y \hat{z}$, and a plane wave dependence in the xz plane for ψ , we get a one-dimensional problem in the y direction. Numerical work again reveals that $k = 0$ for all $\tilde{\mu}$ [42], so the H_{c3} picture is as shown in Fig. 2.

$$C \cdot \hat{n} \cdot \hat{z}, H \cdot k \hat{z}.$$

The high-symmetry geometries are shown in Fig. 5. In this case the field can not orient the SBF. Let us first assume that M^y stays fixed parallel to a \hat{z} , i.e., that the appearance of superconductivity at the surface does not reorient M^y . Now, by the argument of the previous subsection, we expect the same H_{c3} behavior in the two geometries for the E_{2g} and $E_{2u}^{(2)}$ order parameters, and opposite behavior for the the E_1 order parameters.

The two types of behavior, i.e., surface and SBF in concert and opposition, can be seen by studying the E_{1g} case with $\tilde{\mu} < 0$. For Fig. 5 (a) and 5 (b), we have $\psi_x = \psi_y^0 = 0$ at $x = 0$, and $\psi_x^0 = \psi_y = 0$ at $y = 0$ respectively. Since $H \cdot k \hat{z}$, there is no kink in H_{c2} and none is expected in H_{c3} either. The ratio $H_{c3}=H_{c2}$ is still of interest and we have found this numerically. When $\psi_x = 0$, [Fig. 5 (a)], surface superconductivity is not supported in the higher T_c component, and we find, as expected, that $H_{c3} = H_{c2}$. When $\psi_x^0 = 0$, [Fig. 5 (b)], surface superconductivity is supported in the component that onsets first as T is lowered, and $H_{c3} > H_{c2}$. Our results with $u = 0.46$, and $v = 0.1$ are shown in Fig. 6. The ratio $H_{c3}=H_{c2}$ varies from 1.71 for $T = T_{c+}$ to 1.77 for $T = T_{c+} - 2 T_c$.

The assumption of fixed M^y parallel to a \hat{z} may not be physically relevant, however. Since the observed magnitude of M^y is very small [21,22], reorientation of M^y near the surface must be considered. If $M^y \cdot \hat{z}$ near the surface, and $M^y \cdot \hat{z}$ in the bulk, the superconducting

condensation energy could outweigh the magnetic anisotropy and domain wall energies. In this case, we expect a picture resembling Fig. 6 for all the E models for any $\hat{n} \neq \hat{z}$, $H \parallel \hat{z}$.

V. COMPARISON WITH EXPERIMENT, PREDICTIONS, AND CONCLUSIONS

As stated before, Keller et al. have reported [25] surface superconductivity in a whisker of UPt_3 . The long axis of the whisker is along the c -axis of the crystal, and it has six facets along the $h100g$ crystal planes, i.e., the surface normals are $\hat{n} = \hat{x} = \hat{a}$, and five others obtained by successive 60° rotations about \hat{z} . Keller et al. study the ac resistivity and susceptibility for various field orientations, two of which are $H \parallel \hat{a}$ and $H \parallel \hat{c}$, corresponding to the geometries in Figs. 4 (a) and 5 (a) of our paper. The magnitude of the ratio of the critical field to the bulk H_{c2} (1.19 and 1.35 for $H \parallel \hat{a}$), plus the cusp-shaped deviations in the critical field for fields with a small (positive or negative) component along \hat{n} (see Figs. 1 and 2 of their paper), leave little doubt that the observation is indeed of H_{c3} .

Let us begin by studying the case where $H \parallel \hat{a} = \hat{y}$. Recall that $\hat{n} = \hat{x}$. Keller et al. report $H_{c3}=H_{c2} = 1.35$ for $T = 470$ mK. Given that (i) $T_{c+} = 508$ mK, and that the bare T_c splitting $\Delta = 0$, is about 35 mK in the annealed crystals, and (ii) that $H_{c3}=H_{c2}$ decreases to 1.15 and 1.05 for $T = 450$ and 415 mK, respectively, which are above and below the tetracritical temperature, $T = 430$ mK, we tentatively conclude that the H_{c3} curve is of the type shown in Fig. 1, i.e., there is surface superconductivity in only one component, and it onsets at T_{c+} . This picture is obtained within the $A_{1g} B_{2g}$ and $A_{1u} B_{1u}$ models if $T_a > T_b$. Within the $A_{1u} B_{2u}$ model the predicted picture is that of Fig. 3, whether $T_a > T_b$ or $T_b > T_a$. This does not seem to fit the observations, which would appear to exclude the specific $A_{1u} B_{2u}$ order parameter listed in Table I. Within the E models, the picture requires that ϵ_x have the higher T_c when $H \parallel \hat{y}$, i.e. $M^y \parallel \hat{x}$. This in turn requires $\epsilon_x < 0$ for the E_1 models, and $\epsilon_x > 0$ for the E_2 models. These facts are summarized in Table II.

Let us now consider the $H \parallel \hat{c}$, $\hat{n} = \hat{x}$ case. An $H_{c3} > H_{c2}$ is seen at $T = 0.932T_c$ [473

mK . Since data are not given at any other T , the picture of $H_{c3}(T)$ could resemble any of our Figs. 1, 3, or 6. For the AB models we expect the same qualitative behavior as when $H \parallel \hat{a}$, since the direction of H in the plane normal to \hat{n} does not alter the boundary conditions. For any of the four E models ($E_{1g}, E_{2g}, E_{1u}, E_{2u}^{(2)}$), on the other hand, a little work shows that if we assume that M^y stays fixed along \hat{a} , then the sign of χ in Table II is such that for the present geometry the surface and SBF are in opposition. This would imply no surface superconductivity. As argued in Sec. IV C, however, a reorientation of M^y is quite possible, in which case all four E models would lead to an H_{c3} curve as in Fig. 6.

We thus see that the present H_{c3} data can only be used to exclude (and not very confidently at that) the $A_{1u} - B_{2u}$ order parameter in Table I. We can however predict the expected behavior for the other geometries based on the results in Secs. III and IV, given the restrictions in Table II. These predictions are summarized in Table III, which is the main result of our paper.

It can be seen that widely different results are obtained for the geometries $\hat{n} = \hat{c}$ and $\hat{n} = \hat{a}$. The case $\hat{n} = \hat{c}$ distinguishes between E_1 and E_2 models and between E and AB models, if one can confidently detect the presence or absence of a kink in H_{c3} . The case with $\hat{n} = \hat{a}$ and $H \parallel \hat{a}$ distinguishes between the odd and even parity E models, and the AB models. Systematic experimental efforts to study these cases, would be, to state the obvious, extremely valuable. Even for the one surface that is presently available, $\hat{n} = \hat{a}$, studying the variation of H_{c3} with field orientation in the $a-c$ plane would be useful and would improve theoretical study.

ACKNOWLEDGMENTS

We are indebted to W. P. Halperin, Jan Kycia, Jim Sauls, and Sungkit Yip for many illuminating discussions. This work is supported by the National Science Foundation through the Northwestern University Materials Research Center, Grant No. DMR-9120521.

APPENDIX :

We describe here our numerical procedure for finding the matrix of the GL Hamiltonian (4.3), using the case of Sec. IV A for specificity. We denote the operator valued elements of the matrix (4.6) by H_{xx} , H_{xy} , H_{yx} , and H_{yy} , and define

$$H_{ii}^{(0)} = w \partial_z^2 + (1-u)z^2; \quad i = x; y; \quad (A1)$$

We work in the eigenbasis $|j; i\rangle$ of $H_{ii}^{(0)}$:

$$H_{ii}^{(0)} |j; i\rangle = [w(1-u)]^{j=2} (2n+1) |j; i\rangle; \quad i = x; y; \quad n = 0; 1; 2; \dots; \quad (A2)$$

These functions are normalized on the half-space $z > 0$. Depending on the boundary conditions, only even or odd n may be needed.

The matrix representation of H_{GL} in this basis is clearly very simple, except for the following elements:

$$P_{nm} = \langle n; x | j | n; x \rangle; \quad (A3)$$

$$Q_{nm} = \langle n; x | j | n; y \rangle; \quad (A4)$$

$$R_{nm} = \langle n; x | j | n; y \rangle; \quad (A5)$$

We do not need to define $\langle n; y | j | n; y \rangle$ separately, as

$$\langle n; y | j | n; y \rangle = [(1+u)/(1-u)]^{j=4} P_{nm}; \quad (A6)$$

These matrix elements can be found efficiently using the generating function of the Hermite polynomials. We show how this is done for R_{nm} . Note first, that

$$R_{nm} = \int_0^1 \frac{z^{n+m}}{x^2 y^{2n+2m}} \exp\left[-\frac{z^2}{2x} - \frac{z^2}{2y}\right] H_n\left(\frac{z}{x}\right) H_m\left(\frac{z}{y}\right) dz; \quad (A7)$$

where $\int_{xy} = [w(1-u)]^{j=4}$, and H_n is a Hermite polynomial. Denoting the integral in Eq. (A7) by I_{nm} , and using the generating function, we get

$$\begin{aligned} \frac{I_{nm}}{n!m!} &= \int_0^1 z \exp(s^2 + 2sz) \exp(t^2 + 2tz) dz \\ &= \frac{1}{2A} e^{(B^2 - 4AC)/4A} \left[\frac{B}{2A} \operatorname{erfc}\left(\frac{B}{2A}\right) + \operatorname{erfc}^0\left(\frac{B}{2A}\right) \right]; \end{aligned} \quad (\text{A } 8)$$

where $A = (s^2 + t^2)/2$, $B = 2(s + t)$, $C = s^2 + t^2$, and $\operatorname{erfc}^0(x) = \int_0^x \operatorname{erfc}(x) dx$, with

$$\operatorname{erfc}(x) = 1 - \frac{2}{\sqrt{\pi}} x + \frac{x^3}{3} - \frac{x^5}{5 \cdot 2!} + \frac{x^7}{7 \cdot 3!} - \dots; \quad (\text{A } 9)$$

The problem of finding R_{nm} is now reduced to expanding the right hand side of Eq. (A 8) in powers of s and t , and comparing coefficients. This can be done as follows. Consider a polynomial $A(s;t)$, of maximum order $s^N t^M$:

$$A(s;t) = \sum_{n=0}^N \sum_{m=0}^M a_{nm} s^n t^m; \quad (\text{A } 10)$$

The array a_{nm} defines the polynomial. The array for the sum of two polynomials $A(s;t)$ and $B(s;t)$ with arrays a_{nm} and b_{nm} is obviously

$$c_{nm} = a_{nm} + b_{nm}; \quad 0 \leq n \leq N; 0 \leq m \leq M; \quad (\text{A } 11)$$

The product $A(s;t)B(s;t)$ has terms up to order $s^{2N} t^{2M}$. If we are only interested in terms up to order $s^N t^M$, however, we can write the corresponding array as

$$c_{nm} = \sum_{i=0}^n \sum_{j=0}^m a_{ij} b_{n-i, m-j}; \quad 0 \leq n \leq N; 0 \leq m \leq M; \quad (\text{A } 12)$$

Note that only array elements a_{nm} and b_{nm} with $n \leq N, m \leq M$ appear in this formula.

The above procedure can be used to expand the right hand side of Eq. (A 8). Suppose we want I_{nm} for $n, m \leq N$, where N is a number of order 20, say. We write B and C as polynomials in s and t , and represent them by arrays as above. (Most of the elements of these arrays are zero at this stage.) We then Taylor expand $\exp(B^2/4A)$, $\exp(C)$, $\operatorname{erfc}(B/2A)$, and $\operatorname{erfc}^0(B/2A)$, and repeatedly use the array operations (A 11) and (A 12) with $N = M = N$, to evaluate Eq. (A 8). The I_{nm} can be directly read off the resulting array.

REFERENCES

- [1] For a recent theoretical review see J.A. Sauls, *Adv. Phys.* 43, 113 (1994), and references therein.
- [2] For an experimental review, see L. Taillefer, J. Floquet, and G.G. Lonzarich, *Physica* 169B, 257 (1991), and references therein.
- [3] S. Adenwalla et al., *Phys. Rev. Lett.* 65, 2298 (1990).
- [4] G. Bnuls et al., *Phys. Rev. Lett.* 65, 2294 (1990).
- [5] R.A. Fisher et al., *Phys. Rev. Lett.* 62, 1411 (1989).
- [6] N.H. van Dijk et al., *Phys. Rev. B* 48, 1299 (1993).
- [7] K. Hasselbach, L. Taillefer, and J. Floquet, *Phys. Rev. Lett.* 63, 93 (1989).
- [8] S.W. Lin et al., *Phys. Rev. B* 49, 10001 (1994).
- [9] R. Joynt, *Supercond. Sci. Technol.* 1, 210 (1988).
- [10] M. Zhitomirskii, *Pisma Zh. Eksp. Teor. Fiz.* 49, 333 (1989) [*JETP Lett.* 49, 379 (1989)].
- [11] D.W. Hess, T.A. Tokuyasu, and J.A. Sauls, *J. Phys. Condens. Matter* 1, 8135 (1989).
- [12] R. Joynt, V.P. Mineev, G.E. Volovik, and M.E. Zhitomirskii, *Phys. Rev. B* 42, 2014 (1990).
- [13] I. Luk'yanchuk, *J. Phys. I (France)* 1, 1155 (1991).
- [14] Note that D_{6h}^0 is a double group, as is appropriate *prima facie* for a strongly spin-orbit coupled metal such as UPt_3 . Nevertheless, a model that effectively ignores spin-orbit coupling has put forward by K. Machida and M. Ozaki, *Phys. Rev. Lett.* 66, 3293 (1991).
- [15] D.C. Chen and Anupam Garg, *Phys. Rev. Lett.* 70, 1689 (1993).

- [16] Anupam Garg and D. C. Chen, *Phys. Rev. B* 49, 479 (1994).
- [17] V. P. Mineev, *Ann. de Physique* 19, 367 (1994).
- [18] A rather different model based on staggered superconductivity, which we do not study here, has been proposed by R. Heid, Ya. B. Bazaliy, V. M. Artisovits, and D. L. Cox, *Phys. Rev. Lett.* 74, 2571 (1995).
- [19] In the other subclass the parameters have opposite parity and are otherwise unrestricted.
- [20] If the parity is odd, we replace the ψ' s by ψ everywhere.
- [21] G. Aeppli et al, *Phys. Rev. Lett.* 60, 615 (1988).
- [22] A. I. Goldman et al, *Phys. Rev. B* 36, 8523 (1987).
- [23] This failure arises from the presence of gradient terms in the free energy that couple the two order parameter components, and thus lead to level repulsion in the H_{c2} eigenvalue problem. Barring the weak hexagonal Fermi-surface anisotropy argument surrounding Eq. (6.6) of Ref. [16], this problem is also present in the A_1 - A_2 and B_1 - B_2 models examined in Ref. [17], which admit a term $iH_z(\psi_1\psi_2 - \psi_2\psi_1)$ in the free energy, where ψ_1 and ψ_2 are the two order parameter components.
- [24] We do not consider paramagnetic corrections such as those embodied in Eq. (19) of Ref. [1].
- [25] N. Keller, J. L. Tholence, A. Huxley, and J. Floquet, *Phys. Rev. Lett.* 73, 2364 (1994); 74, 2148 (1995) (E).
- [26] K. V. Samokhin, *Zh. Eksp. Teor. Fiz* 107, 906 (1995) [*Sov. Phys. JETP* 80, 515 (1995)].
- [27] See also Yu. S. Barash, A. V. Galaktionov, and A. A. Svidzinsky (to be published).
- [28] P. G. de Gennes, *Superconductivity of Metals and Alloys* (Addison-Wesley, New York, 1989).

- [29] D. Saint-James, G. Sarma, and E. J. Thomas, *Type II Superconductivity* (Pergamon 1969).
- [30] D. Saint-James and P. G. de Gennes, *Phys. Lett.* **7**, 306 (1963).
- [31] V. Ambegaokar, P. G. de Gennes, and D. Rainer, *Phys. Rev. A* **9**, 2627 (1974).
- [32] More generally, the condition is $\hat{n}^{\$} D = M$, where the matrix M is a generalization of the inverse extrapolation length for s-wave superconductors, and $\hat{n}^{\$}$ is a tensor both with respect to cartesian indices x, y, z , and order parameter component indices. The volume integral of $f_{GL}^{(2)}$ should be a hermitian quadratic form; this condition requires $M = M^{\dagger}$. The vanishing of $\hat{n}^{\$}_{ij}$ then follows automatically. See also Ref. [26].
- [33] Sungkit Yip and Anupam Garg, *Phys. Rev. B* **48**, 3304 (1993).
- [34] The general gap function is a linear combination of 'crystal harmonics' and need not have definite orbital angular momentum. The examples in Table I suggest otherwise and may be too simplistic in this regard.
- [35] M. Norman, *Physica C* **194**, 203 (1992).
- [36] T. Tokuyasu, Ph.D. thesis, Princeton University, 1990 (unpublished)].
- [37] Anupam Garg, *Phys. Rev. Lett.* **69**, 676 (1993).
- [38] J. A. Sauls (to be published).
- [39] D. F. Agterberg and M. B. Walker, *Phys. Rev. Lett.* **74**, 3904 (1995).
- [40] N. Keller, J. L. Tholence, A. Huxley, and J. Flouquet, *Phys. Rev. Lett.* **74**, 3905 (1995).
- [41] We obtain the same answers using Weber functions for x and y .
- [42] We have not investigated the onset of k -mixing as u is changed.

FIGURES

FIG . 1. Schematic behavior of $H_{c3}(T)$ when only the higher T_c order-parameter component supports surface superconductivity.

FIG . 2. Same as Fig. 1, when only the lower T_c component supports surface superconductivity.

FIG . 3. Same as Fig. 1, when both components support surface superconductivity. In this case we expect inner H_{c3} lines (dot-dashed) near the kink in H_{c3} . We have not explicitly calculated these lines.

FIG . 4. High symmetry geometries when $\hat{n} \parallel \hat{z}$, $H \parallel \hat{z} \parallel \hat{n}$. a , a , and c are the crystal axes.

FIG . 5. Same as Fig. 4 for $\hat{n} \parallel \hat{z}$, $H \parallel \hat{z}$.

FIG . 6. Behavior of $H_{c3}(T)$ in the E models for $\hat{n} \parallel \hat{z}$, $H \parallel \hat{z}$, when the higher T_c component supports surface superconductivity. The dot-dashed line is the ratio H_{c3}/H_{c2} . The curves shown are calculated for $u = 0.46$, $v = 0.1$.

TABLES

TABLE I. Boundary conditions for various candidate order parameters for UPt_3 . The last three columns list the pair of quantities that must vanish at the surface for given surface normal \hat{n} . Note that (i) a prime denotes a normal derivative, (ii) the axes \hat{x} , \hat{y} , and \hat{z} are fixed along the crystal symmetry axes a , a' , and c , respectively.

Representation	r or \tilde{r}	Quantities that vanish for		
		$\hat{n} = \hat{z}$	$\hat{n} = \hat{x}$	$\hat{n} = \hat{y}$
E_{1g}	$(k_z k_x; k_z k_y)$	$(1; 2)$	$(1; 0)$	$(0; 2)$
E_{2g}	$(k_x^2 - k_y^2; 2k_x k_y)$	$(0; 0)$	$(0; 2)$	$(0; 2)$
E_{1u}	$(k_x; k_y) \hat{z}_s$	$(0; 0)$	$(1; 0)$	$(0; 2)$
$E_{2u}^{(1)}$	$(k_x \hat{x}_s - k_y \hat{y}_s; k_x \hat{y}_s + k_y \hat{x}_s)$	$(0; 0)$	Mixed	Mixed
$E_{2u}^{(2)}$	$(k_x^2 - k_y^2; 2k_x k_y) k_z \hat{z}_s$	$(1; 2)$	$(0; 2)$	$(0; 2)$
$A_{1g} \quad B_{2g}$	$(1; k_x^3 k_z - 3k_x k_y^2 k_z)$	$(0; 2)$	$(0; 2)$	$(0; 0)$
$A_{1u} \quad B_{2u}$	$(k_z; 3k_x^2 k_y - k_y^3) \hat{z}_s$	$(1; 0)$	$(0; 0)$	$(0; 2)$
$A_{1u} \quad B_{1u}$	$(k_z; 3k_x k_y^2 - k_x^3) \hat{z}_s$	$(1; 0)$	$(0; 2)$	$(0; 0)$

TABLE II. Constraints on the transition temperatures, or the sign of the coupling to the symmetry breaking field, for the order parameters listed in Table I, obtained by requiring agreement with the H_{c3} data of Keller et al. for $H \parallel \hat{a}$, $\hat{n} \parallel \hat{a}$.

Order parameter	Constraint
$A_{1g} \quad B_{2g}$	$T_a > T_b$
$A_{1u} \quad B_{2u}$	No agreement
$A_{1u} \quad B_{1u}$	$T_a > T_b$
E_{1g} or E_{1u}	< 0
E_{2g} or $E_{2u}^{(2)}$	> 0

TABLE III. Expected H_{c3} vs. T behavior for the principal geometries. The order parameters for each case are as in Table I, and the signs of $(T_a - T_b)$ and \hat{n} are as in Table II. A blank denotes a case that we have not studied. No SSC' stands for no surface superconductivity.

Order parameter	$\hat{n} = \hat{c}$	$\hat{n} = \hat{a}$	$\hat{n} = \hat{a}$	$\hat{n} = \hat{a}$	$\hat{n} = \hat{a}$
	$H \sim \hat{c}$	$H \sim \hat{a}$	$H \sim \hat{a}$	$H \sim \hat{c}$	$H \sim \hat{c}$
E_{1g}	No SSC	Fig. 1	Fig. 1	Fig. 6 ^a	Fig. 6
E_{2g}	Fig. 3	Fig. 1	Fig. 2	Fig. 6 ^a	Fig. 6 ^a
E_{1u}	Fig. 3	Fig. 1	Fig. 1	Fig. 6 ^a	Fig. 6
$E_{2u}^{(1)}$	Fig. 3				
$E_{2u}^{(2)}$	No SSC	Fig. 1	Fig. 2	Fig. 6 ^a	Fig. 6 ^a
$A_{1g} \quad B_{2g}$	Fig. 1	Fig. 1	Fig. 3	Fig. 1	Fig. 3
$A_{1u} \quad B_{2u}$	Fig. 2 ^b	Fig. 3	Fig. 1 ^c	Fig. 3	Fig. 1 ^c
$A_{1u} \quad B_{1u}$	Fig. 2	Fig. 1	Fig. 3	Fig. 1	Fig. 3

a. Assuming that the surface reorients M^y . Otherwise no surface superconductivity is expected.

b. Assuming $T_a > T_b$. Otherwise Fig. 1 applies.

c. Assuming $T_a > T_b$. Otherwise Fig. 2 applies.

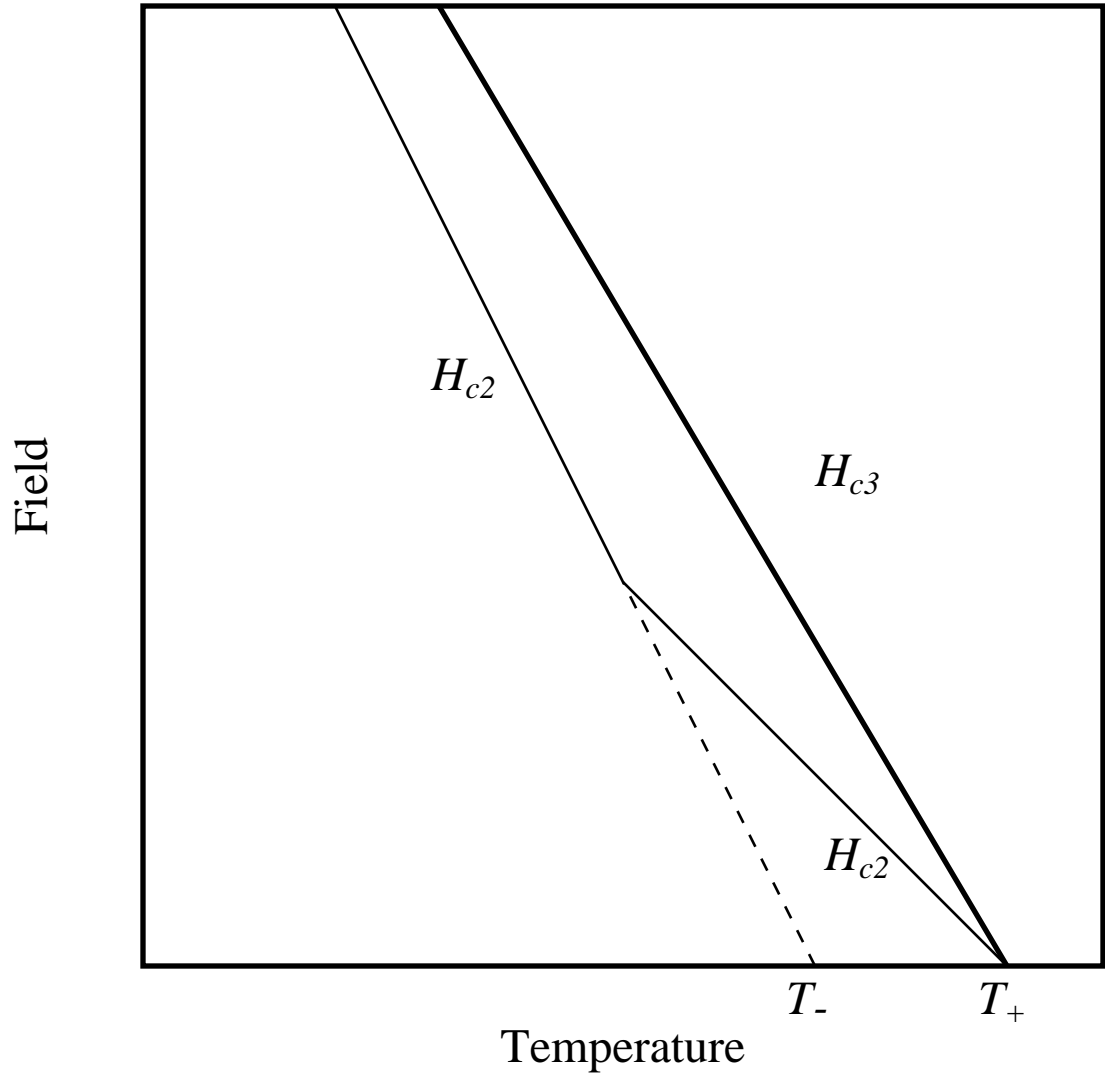


Fig. 1

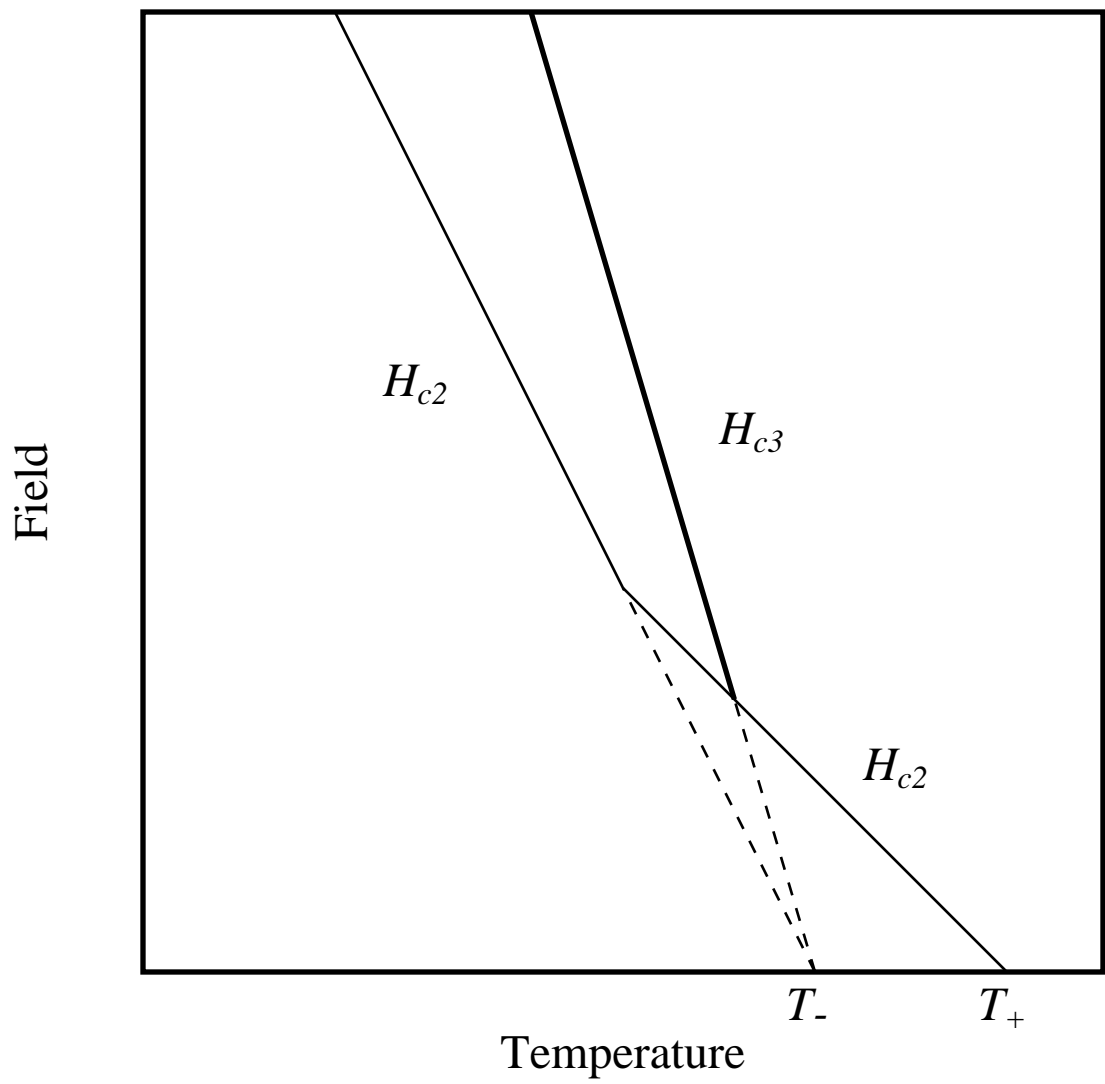


Fig. 2

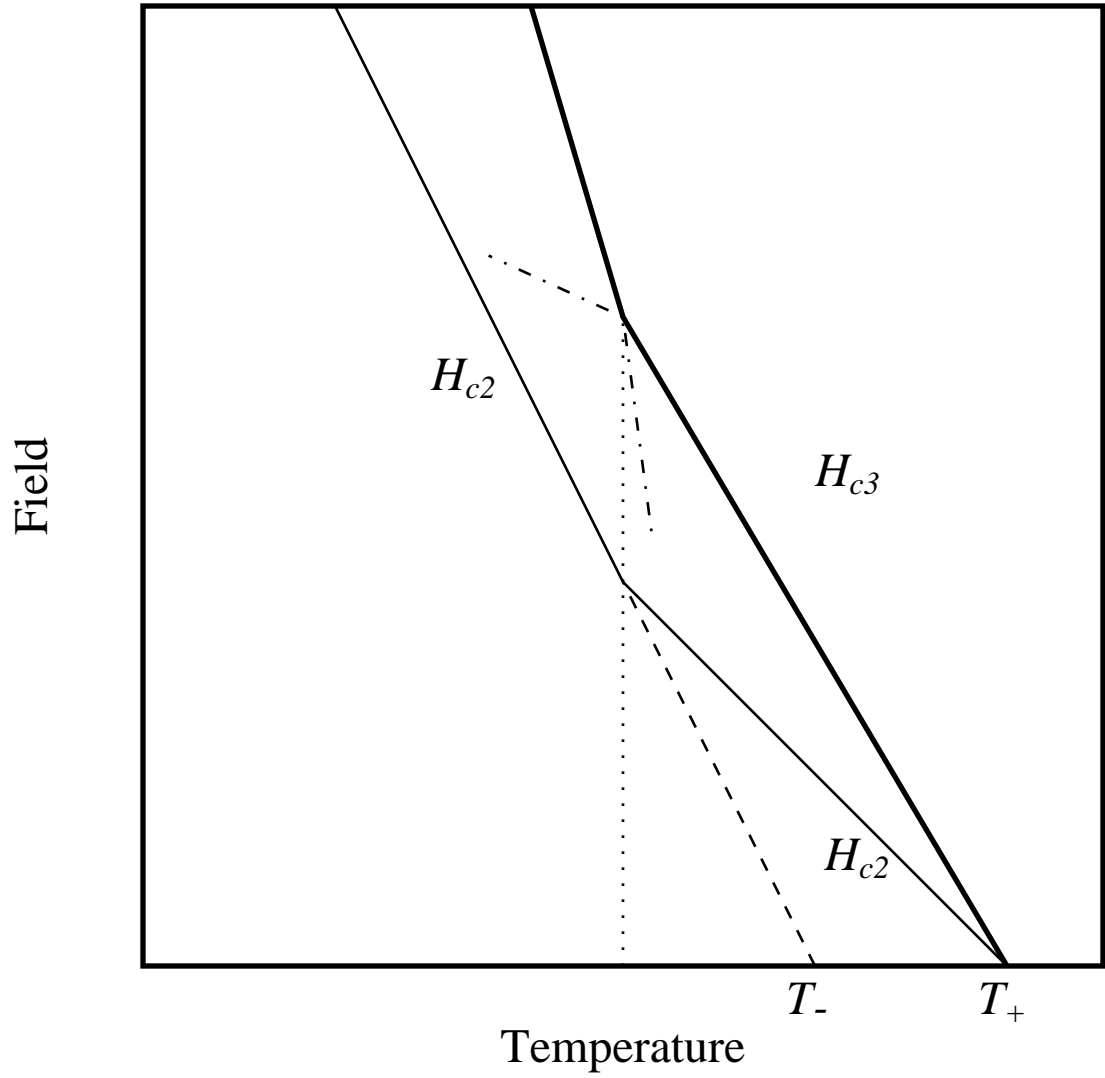


Fig. 3

Fig. 4

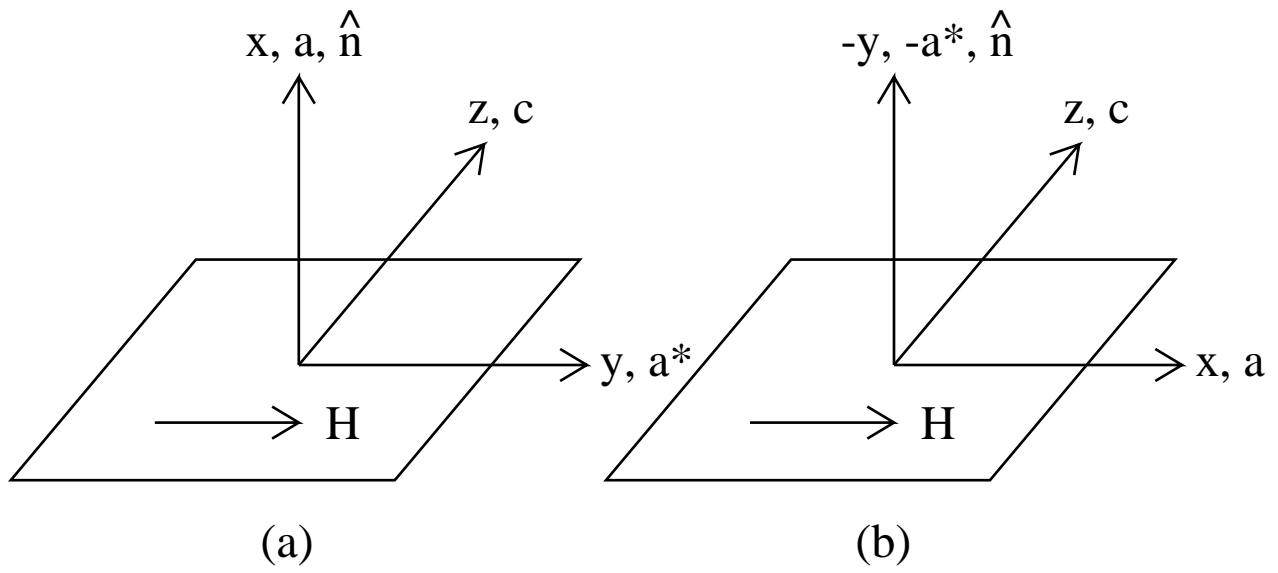
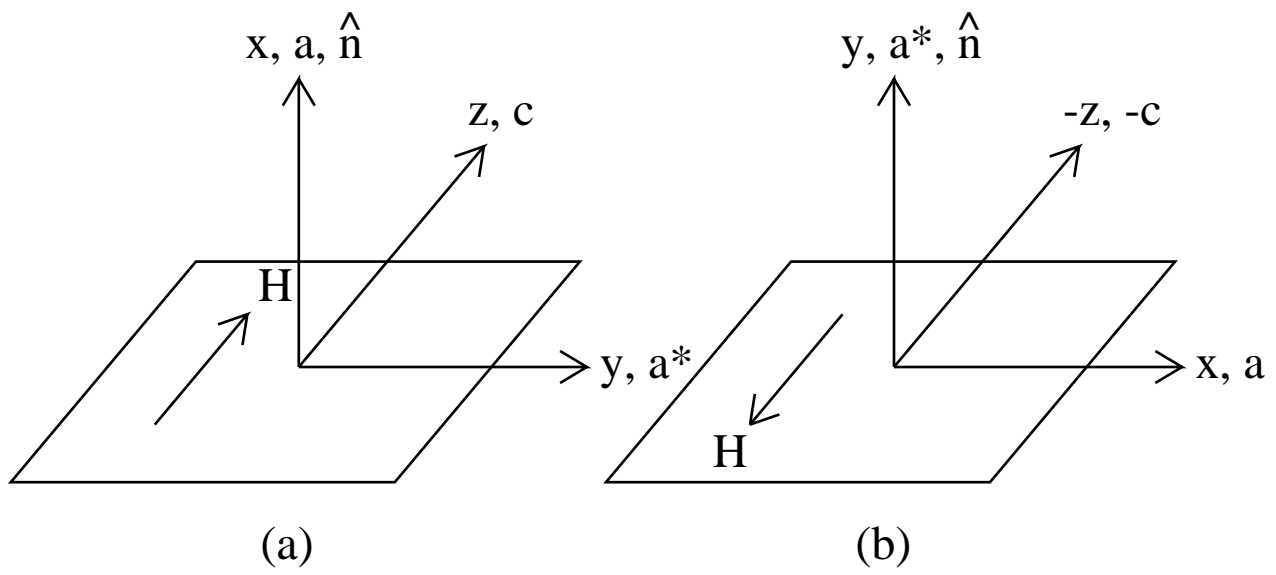


Fig. 5



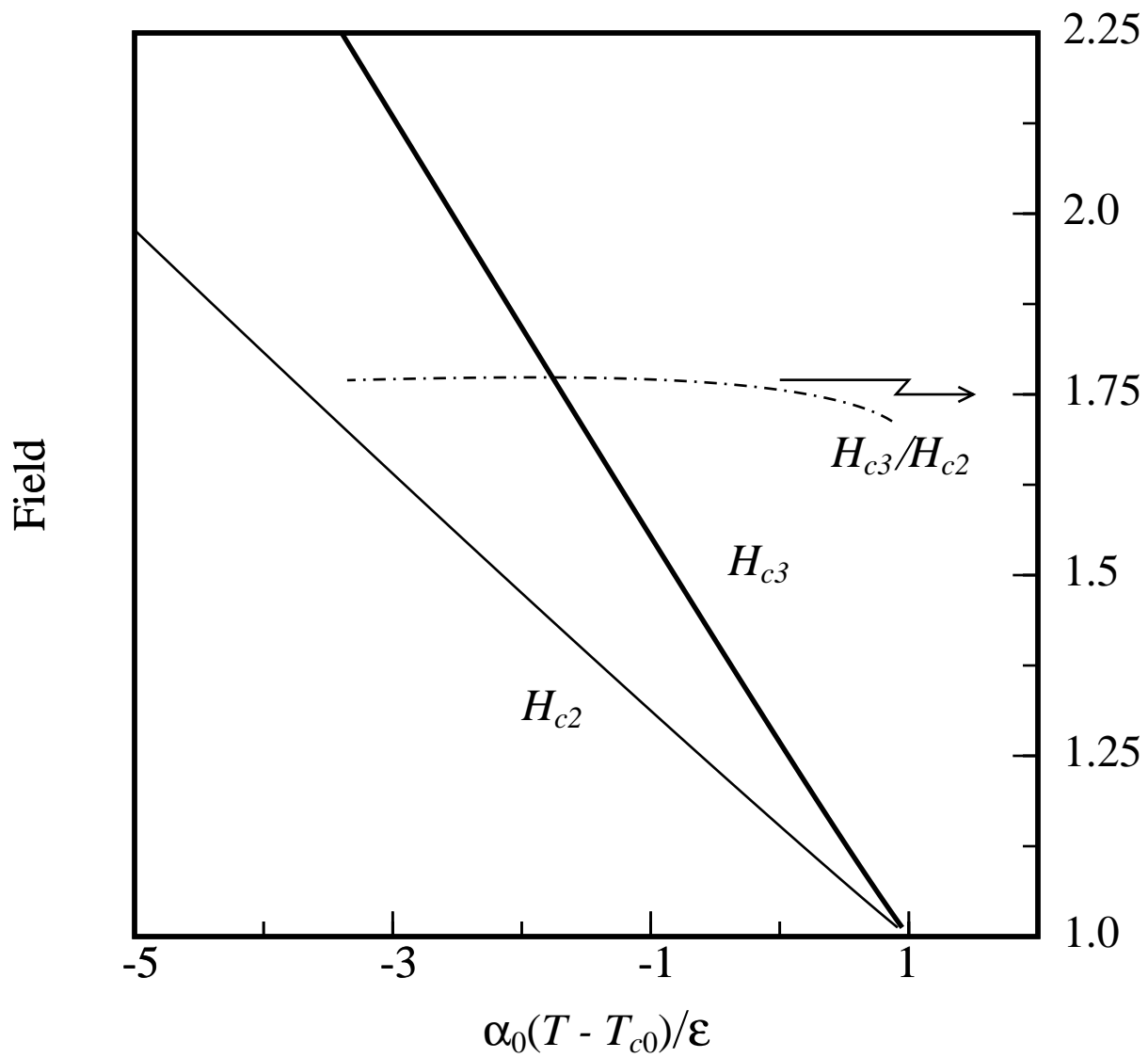


Fig. 6